OPEN

Citation: Cell Death and Disease (2013) 4, e810; doi:10.1038/cddis.2013.330

www.nature.com/cddis

The HDAC inhibitor, MPT0E028, enhances erlotinib-induced cell death in EGFR-TKI-resistant NSCLC cells

M-C Chen[1], C-H Chen[1], J-C Wang[2], A-C Tsai[1], J-P Liou*[,3], S-L Pan*[,2] and C-M Teng*[,1]

Epidermal growth factor receptor (EGFR), which promotes cell survival and division, is found at abnormally high levels on the surface of many cancer cell types, including many cases of non-small cell lung cancer. Erlotinib (Tarceva), an oral small-molecule tyrosine kinase inhibitor, is a so-called targeted drug that inhibits the tyrosine kinase domain of EGFR, and thus targets cancer cells with some specificity while doing less damage to normal cells. However, erlotinib resistance can occur, reducing the efficacy of this treatment. To develop more effective therapeutic interventions by overcoming this resistance problem, we combined the histone deacetylase inhibitor, MPT0E028, with erlotinib in an effort to increase their antitumor effects in erlotinib-resistant lung adenocarcinoma cells. This combined treatment yielded significant growth inhibition, induced the expression of apoptotic proteins (PARP, γH2AX, and caspase-3), increased the levels of acetylated histone H3, and showed synergistic effects *in vitro* and *in vivo.* These effects were independent of the mutation status of the genes encoding EGFR or K-Ras. MPT0E028 synergistically blocked key regulators of the EGFR/HER2 signaling pathways, attenuating multiple compensatory pathways (e.g., AKT, extracellular signal-regulated kinase, and c-MET). Our results indicate that this combination therapy might be a promising strategy for facilitating the effects of erlotinib monotherapy by activating various networks. Taken together, our data provide compelling evidence that MPT0E028 has the potential to improve the treatment of heterogeneous and drug-resistant tumors that cannot be controlled with single-target agents.
Cell Death and Disease (2013) **4,** e810; doi:10.1038/cddis.2013.330; published online 19 September 2013
Subject Category: Cancer

Epidermal growth factor receptor (EGFR) belongs to a superfamily of receptor tyrosine kinases (RTKs) that mediate cell signaling by extracellular growth factors to promote cell proliferation and survival.[1] Altered expression of the EGFR has been found in a variety of human malignancies, including lung, breast, and ovarian cancers.[2] Non-small cell lung carcinoma (NSCLC) is characterized by the accumulation of multiple genetic alterations and comprises diverse histological subtypes.[3,4] EGFR-mutant NSCLC was defined as a unique and clinically relevant subset of lung cancer.[5] Most patients with advanced NSCLC have unfavorable prognosis and low survival rates at the time of diagnosis.[6] Combined treatment with chemotherapeutic agents has resulted in a modest increase in survival, but these treatments cause significant toxicity to patients.[7]

The tyrosine kinase inhibitor (TKI), erlotinib (OSI-774, Tarceva; OSI Pharmaceuticals/Genentech, New York, NY, USA), is an oral small-molecule inhibitor that binds to the kinase domain of EGFR and was approved for the treatment of NSCLC in 2004. The introduction of this targeted therapeutic agent generated a great deal of optimism, especially among patients with activating (drug-sensitive) EGFR mutations, a non-smoking history, female gender, and Asian origin, all of which have been associated with a higher probability of response to TKIs.[8,9] Despite an initial dramatic response to such inhibitors, however, most patients ultimately developed drug resistance, followed by relapse.[10] Several clinical studies have shown that a secondary point mutation at amino-acid position 790 (T790M) of EGFR is responsible for approximately half of the cases in which patients with lung adenocarcinoma develop resistance to EGFR-targeting TKIs.[10,11] In addition, the presence of an intrinsic (primary) resistance mechanism (such as K-Ras mutation) can also confer resistance to TKIs, although the underlying mechanisms are not yet completely understood.[12] Thus, the identification of alternative approaches that further disrupt

[1]Pharmacological Institute, College of Medicine, National Taiwan University, Taipei, Taiwan; [2]The PhD Program for Cancer Biology and Drug Discovery, College of Medical Science and Technology, Taipei Medical University, Taipei, Taiwan and [3]School of Pharmacy, College of Pharmacy, Taipei Medical University, Taipei, Taiwan
*Corresponding author: J-P Liou, School of Pharmacy, College of Pharmacy, Taipei Medical University, No. 250, Wu-hsing Street, Taipei 11031, Taiwan. Tel: +886 2 2736 1661, Ext 6130; Fax: +886 2 2736 9558; E-mail: jpl@tmu.edu.tw
or S-L Pan, The PhD Program for Cancer Biology and Drug Discovery, College of Medical Science and Technology, Taipei Medical University, 250 Wu-hsing Street, Taipei 11031, Taiwan. Tel: +886 2 2736 1661, Ext 7671; Fax: +886 2 2322 1742; E-mail: slpan@tmu.edu.tw
or C-M Teng, Pharmacological Institute, College of Medicine, National Taiwan University, No. 1, Sector 1, Jen-Ai Road, Taipei 10051, Taiwan. Tel: +886 2 2312 3456 Ext 88310; Fax: +886 2 2322 1742; E-mail: cmteng@ntu.edu.tw
Keywords: lung cancer; HDAC; synergistic; EGFR; apoptosis; erlotinib
Abbreviations: EGFR, epidermal growth factor receptor; HDAC, histone deacetylase; TKI, tyrosine kinase inhibitor; NSCLC, non-small cell lung cancer; ERK, extracellular signal-regulated kinase; RTK, receptor tyrosine kinase
Received 19.4.13; revised 28.7.13; accepted 31.7.13; Edited by M Agostini

EGFR-dependent tumor cell growth is critical, and such strategies could have significant clinical impacts.

Histone deacetylase (HDAC) inhibitors have been reported to induce a range of anticancer effects, including tumor cell apoptosis, cell cycle arrest, differentiation, senescence, modulation of immune responses, and altered angiogenesis.[13] Several lines of evidence have suggested that combined treatments involving HDAC inhibitors plus TKIs could have synergistic effects in cancer cells.[14–16] Vorinostat (also known as SAHA; suberoylanilide hydroxamic acid), which is the only HDAC inhibitor currently approved as a cancer therapeutic, is used in the clinic to treat cutaneous T-cell lymphoma. In addition, a number of ongoing clinical trials are assessing the combined use of SAHA and erlotinib in patients with advanced NSCLC.[17] Recently, we identified MPT0E028 (3-(1-benzenesulfonyl-2,3-dihydro-1H-indol-5-yl)-*N*-hydroxy-acrylamide; structure shown in Figure 1c) as a novel potent pan-HDAC inhibitor for use in human tumor cell lines.[18]

In this study, we sought to exploit the antitumor activities of MPT0E028 by testing the hypothesis that treatment with erlotinib in combination with MPT0E028 will overcome the resistance to EGFR inhibitors in erlotinib-resistant lung adenocarcinoma cells. Our results revealed that the combined treatment had synergistic effects on cell viability and the activations of poly-ADP-ribose polymerase (PARP) and caspase 3 (markers of apoptosis). Similar effects, along with suppression of tumor growth, were observed in an *in vivo* xenograft model of EGFR inhibitor-resistant NSCLC. These results indicate that a practical approach to creating multi-target anticancer agents based on a single small molecule could significantly enhance the success of cancer therapy.

Results

Cell lines, EGFR status, and inhibition of cell survival by MPT0E028 and erlotinib. We previously tested the growth-inhibiting activity of the HDAC inhibitor, MPT0E028, in a diverse panel of cultured NCI-60 human cancer cell lines,[18] and found that the compound is effective against a broad range of cancer cell types, including lung, ovarian, colon, breast, prostate, and renal cancer cells. In this study, we examined the effects of erlotinib plus MPT0E028 in erlotinib-resistant NSCLC cells with different EGFR characteristics.[19–22]

According to previous studies, the plasma steady-state concentrations of erlotinib in patients with advanced solid tumors reached around 4 μM following a daily dose of 150 mg.[23,24] Thus, we classified cell lines with IC_{50} values higher than 4 μM as erlotinib resistant. As expected, the IC_{50} values (μM) of erlotinib were >10 μM in cell lines that were known to have primary (A549, H1299) or secondary (H1975, CL97, and PC9/IR) resistance to erlotinib (Table 1). In contrast, the erlotinib-resistant cells were sensitive to MPT0E028, which dose-dependently reduced their viability (Figure 1d). Table 1 summarizes the molecular characteristics and cytotoxicities of erlotinib (Figure 1a), vorinostat (SAHA; Figure 1b), and MPT0E028 (Figure 1c) in the five tested human NSCLC cell lines. These cell lines exhibited differential sensitivities to the cytotoxic effects of MPT0E028 and SAHA, and these were unrelated to their EGFR status (wild-type or resistant mutations; Figure 1d and Table 1).

Cytotoxic synergism of erlotinib and MPT0E028. To evaluate the interaction between erlotinib and MPT0E028, the cytotoxicities of MPT0E028 and erlotinib alone or in

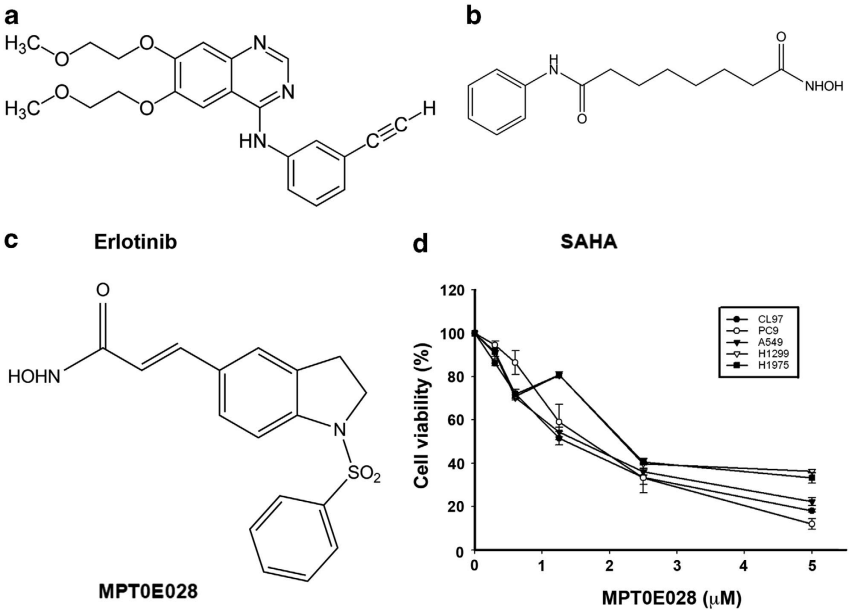

Figure 1 Chemical structures and cytotoxicity of MPT0E028. Chemical structures of erlotinib (**a**), vorinostat/SAHA (**b**), and MPT0E028 (**c**). (**d**) Effects of MPT0E028 on the viability of A549, H1299, H1975, CL97, and PC9/IR cells. Cells were treated with the indicated drugs for 72 h and cell viability was determined by the MTT assay, as described in the Materials and Methods section. Results are representative of at least three independent experiments

Table 1 Molecular characteristics and cytotoxicity of MPT0E028 and erlotinib

Cell line	Characters	E028 (IC_{50})	SAHA (IC_{50})	Erlotinib (IC_{50})
A549	K-Ras mut, EGFR wt	1.55 ± 0.14	8.98 ± 0.24	>20
H1299	EGFRwt, N-RAS (Q61K)	1.1 ± 0.02	5.25 ± 0.38	>20
NCI-H1975	EGFR mut T790M	1.3 ± 0.13	5.34 ± 0.15	>20
PC9/IR	EGFR exon 19 del, activating mut	1.66 ± 0.41	5.32 ± 0.44	>20
CL97	EGFR mut T790M, G719A	1.35 ± 0.11	4.57 ± 0.35	>20

Abbreviations: Del, deletion; Mut, mutant; WT, wild-type.
Cytotoxicity of erlotinib, MPT0E028 or SAHA, and the mutation status of the EGFR and K-Ras genes in human NSCLC cell lines are shown. The cytotoxicities of erlotinib, MPT0E028, or SAHA were determined by MTT assays after 72 h of drug treatment, and are expressed as the IC_{50} (μM). Each value represents the mean $\pm$ standard deviation (S.D.) from at least three independent experiments.

combination were assessed in the five erlotinib-resistant lung adenocarcinoma cells lines (A549, H1299, PC9/IR, CL97, and H1975). Cells were treated with increasing concentrations of erlotinib and/or MPT0E028 for 72 h, and growth inhibition was measured by MTT assay. Compared with erlotinib or MPT0E028 alone, all cells treated with erlotinib plus MPT0E028 exhibited decreased viability (Figures 2a–e). The combination index (CI) values were all <1, indicating that there was a synergistic interaction between erlotinib and MPT0E028 in these five erlotinib-resistant NSCLC cell lines, which differed in their EGFR status. A long-term clonogenicity assay was carried out to assess the capacity of erlotinib plus MPT0E028 to cause irreversible growth arrest in A549 cells. We observed decreases in the colony-forming capacities of the cells (Figure 2f), indicating irreversible growth arrest. Taken together, those findings indicate that the HDAC inhibitor, MPT0E028, can enhance the cell-killing effects of erlotinib in resistant NSCLC cells.

Cell cycle effects of MPT0E028 and erlotinib. Flow cytometry was used to analyze the cell cycle distribution in A549 cells exposed to HDAC inhibitors (MPT0E028 and SAHA), erlotinib alone, or erlotinib plus MPT0E028 or SAHA for 72 h. Treatment with erlotinib alone did not significantly alter the percentage of cells in sub-G1 phase (indicative of apoptosis) compared with control cells (Figure 3a). However, MPT0E028 and erlotinib co-treatment synergistically induced the apoptotic subG1 population in A549 cells. As shown in Figures 3a and b, erlotinib plus MPT0E028 induced apoptosis in 71.7% of A549 cells compared with 10.05% in cells treated with erlotinib alone and 18.73% among those treated with MPT0E028 alone. Synergy was also observed in cells treated with SAHA plus erlotinib, but a higher concentration of SAHA was needed, indicating that it was less potent in this context (Figure 3c). Together, these data revealed that HDAC inhibitors could sensitize resistant A549 cells to the cytotoxic effects of erlotinib.

MPT0E028 plus erlotinib induces apoptosis in NSCLC cells. Our DNA fragmentation ELISA indicated that co-treatment of cells with MPT0E028 plus erlotinib for 72 h significantly and dose-dependently increased the extent of nucleosome formation (a marker of apoptosis) compared with cells treated with each drug alone (Figure 4a). Moreover, the inductions of DNA double-strand breaks and apoptosis were assessed by western blotting for γH2AX induction and the activation of apoptotic proteins (caspase-3 and PARP), respectively. Our results revealed that co-treatment with erlotinib and MPT0E028 synergistically increased the levels of apoptotic proteins in TKI-resistant PC9/IR and CL97 cells (in which resistance is mediated by different mechanisms) when compared with cells treated with either agent alone (Figures 4b and c). Next, we compared MPT0E028 (Figure 4d, left panel) and SAHA (Figure 4d, right panel) in combination with erlotinib for the treatment of primary-resistant NSCLC A549 cells. Combined synergistic effects were seen for both erlotinib/SAHA and erlotinib/MPT0E028, but the latter induced greater γH2AX induction, PARP cleavage, and caspase 3 activation. Interestingly, our western blot analysis revealed greater histone H3 acetylation in samples treated with MPT0E028 plus erlotinib compared with cells treated with either drug alone (Figure 4d, left panel), suggesting that erlotinib and MPT0E028 have a synergistic epigenetic interaction in A549 cells. Notably, the synergistic effects were less prominent when cells were exposed to even higher concentrations of SAHA and erlotinib (Figure 4d, right panel). Overall, our results indicate that MPT0E028 performed better than SAHA in improving the response of resistant cells to the tyrosine kinase inhibitor, erlotinib.

Effect of erlotinib plus MPT0E028 on different models of erlotinib resistance. To further evaluate the enhanced effects of our combined treatment, the protein expression of EGFR and the activation of its downstream signaling proteins, AKT and extracellular signal-regulated kinase (ERK), were analyzed by western blotting. In A549 cells, MPT0E028 or erlotinib alone minimally inhibited the protein levels of phospho-EGFR, phospho-ERK, and phospho-Akt (Figure 5a). In contrast, erlotinib/MPT0E028 co-treatment significantly reduced the levels of phosphorylated-EGFR, EGFR, and the downstream signaling proteins (Figure 5a). Although erlotinib alone dose-dependently induced phosphorylated-ERK and phosphorylated-Akt protein levels in A549 cells, co-treatment with MPT0E028 blocked the inductions of these proteins (Figure 5a). Furthermore, erlotinib/MPT0E028 co-treatment was also found to down-regulate EGFR protein levels in PC9/IR and CL97 cells, which represent resistance acquired through different mechanisms (the latter harbors an EGFR-T790M mutation; Figure 5b). To examine the potential mechanisms of the observed synergy, we examined investigated the effects of MPT0E028 plus erlotinib on the protein levels of other RTKs that have been associated with lung cancer treatment resistance and response, including HER2, IGF-IR, and c-Met.[25–27] As shown in Figure 5c, A549 cells treated with

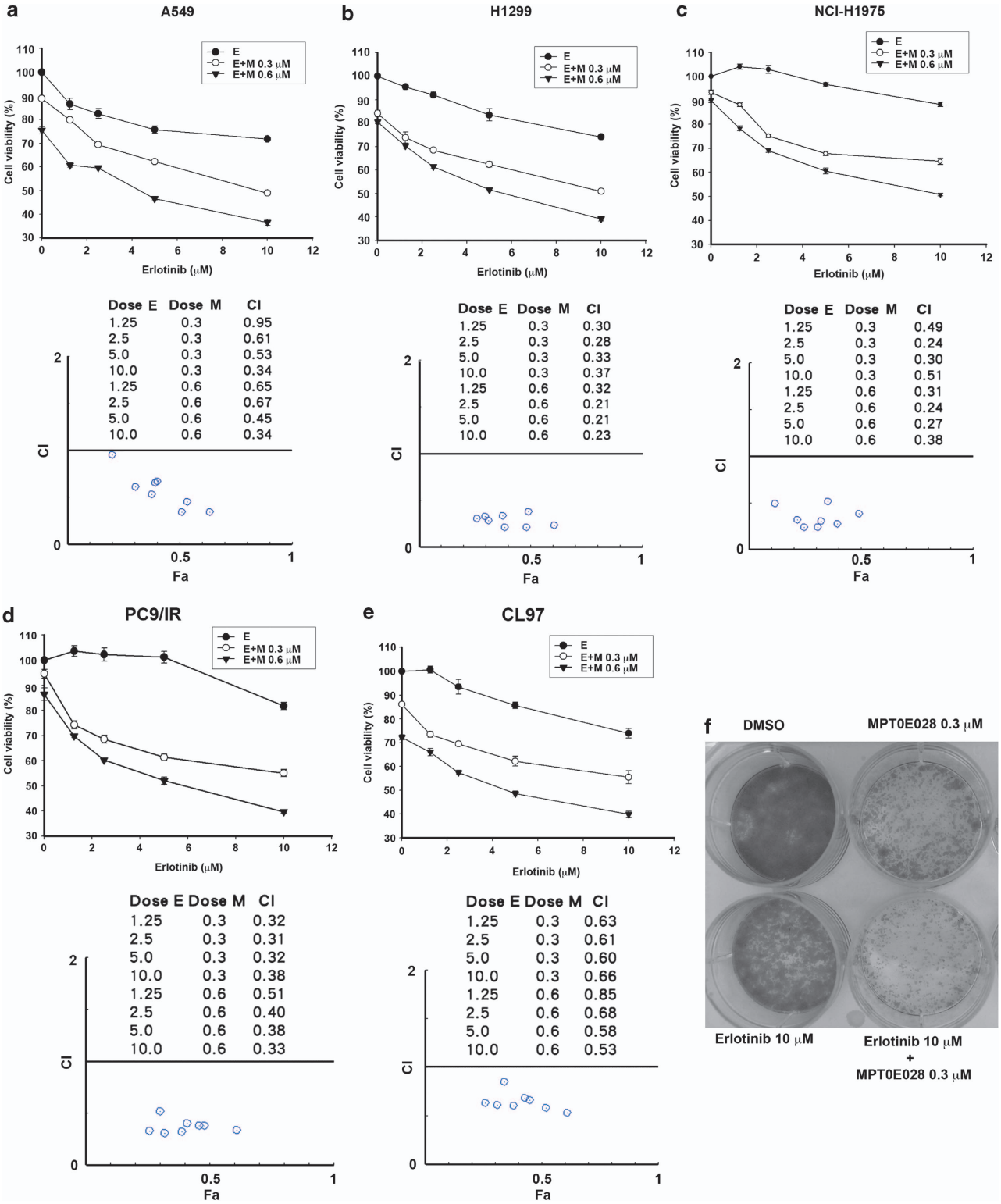

Figure 2 MPT0E028 enhances EGFR inhibitor-induced cytotoxicity in erlotinib-resistant NSCLC cells. Erlotinib-resistant A549 (**a**), H1299 (**b**), H1975 (**c**), PC9/IR (**d**), and CL97 (**e**) cells were incubated with increasing concentrations of erlotinib (E) and MPT0E028 (M) alone or concurrently for 72 h. (**f**) MPT0E028 and erlotinib together synergistically suppress colony formation. Clonogenic survival was assessed as described in the Materials and Methods section, and cell viability was determined by MTT assay. The results are expressed as the percentage surviving cells in drug-treated cultures relative to DMSO-treated control cells. Error bars represent S.D. CI values for the combination of erlotinib and MPT0E028 were calculated using the Calcusyn software (Cambridge, UK), as described in the Materials and Methods section

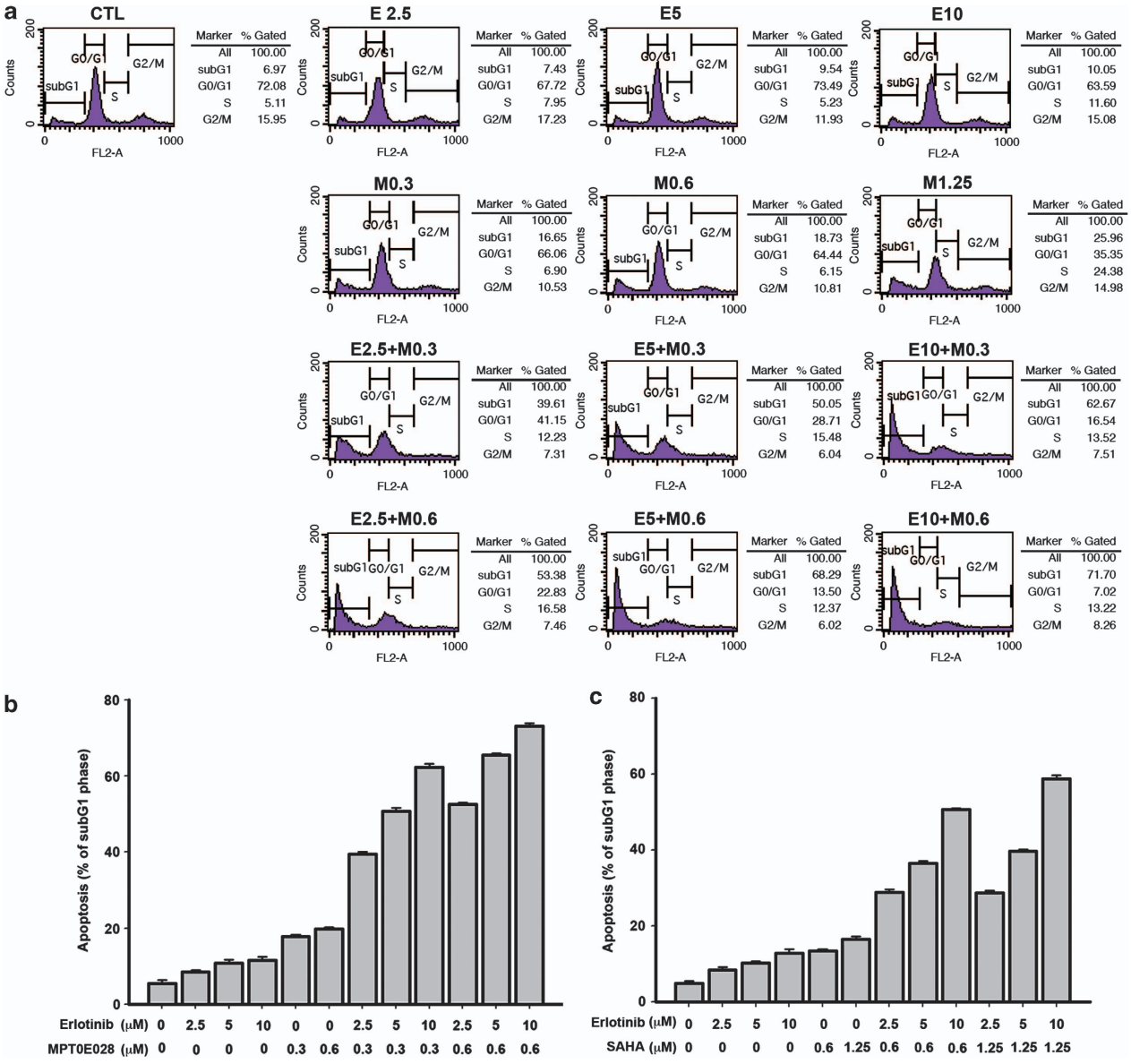

Figure 3 Assessment of apoptosis by propidium iodide in A549 cells. (**a**) Induction of apoptosis (subG1 phase) in A549 cells treated with MPT0E028 (M) in combination with erlotinib (E). Cells were treated with the indicated concentrations (μM) for 72 h, stained with propidium iodide, and assessed by flow cytometry. (**b** and **c**) The percentage of cells in sub-G1 at 72 h after treatment with erlotinib/MPT0E028 (**b**) or erlotinib/SAHA (**c**). Data are representative of the results from at least three independent experiments. Error bars represent S.D.

erlotinib and MPT0E028 showed significant reductions in phospho-c-Met, phospho-IGF-IR, and phospho-HER-2, presumably due to HDAC inhibition. These results indicate the combined treatment potentiate the effects of erlotinib and blocks the tyrosine kinase receptors that have key roles in the pro-oncogenic signaling of lung cancer.

The role of EGFR in the combination with erlotinib and MPT0E028 in EGFR inhibitor-resistant NSCLC cells. We further examined the effect of combined erlotinib and MPT0E028 treatment on EGFR mRNA expression. Interestingly, EGFR mRNA level was upregulated at low concentrations (0.3 μM) and downregulated at higher concentration (1.25 μM) of MPT0E028 in A549 cells, showing biphasic effect in response to MPT0E028 (Figure 6a). However, the induction of EGFR mRNA observed with MPT0E028 treatment in A549 cells was abolished in the combination with erlotinib (Figure 6a) and the mRNA expression pattern paralleled that of the protein expression shown in Figure 5a, suggesting erlotinib/MPT0E028 reduced EGFR through transcriptional regulation. To elucidate whether the downregulation of EGFR represented a major underlying antitumor mechanism for the combination treatment, we assessed the effect of the ectopic expression of EGFR by transiently transfecting A549 and PC9/IR cells with Flag-EGFR plasmids. This ectopic EGFR expression provided a significant protection against the suppression of cell viability and induction of apoptosis in combination with erlotinib and

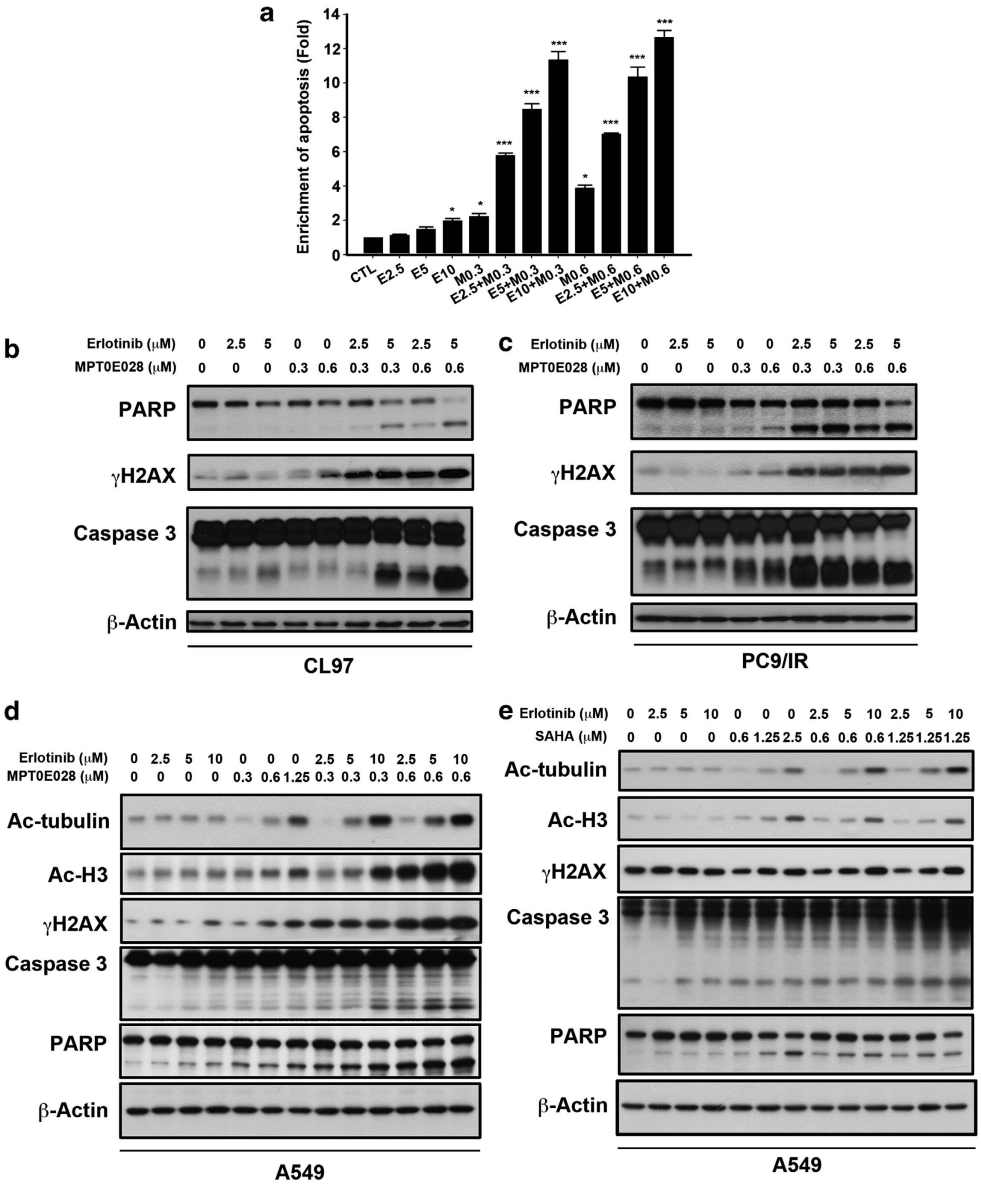

Figure 4 MPT0E028/erlotinib co-treatment induces acetylated histone and non-histone proteins and upregulates apoptotic proteins in lung adenocarcinoma cells. (**a**) Effect of erlotinib/MPT0E028 co-treatment on drug-induced DNA fragmentation in A549 cells. Cells were treated with the indicated concentrations of MPT0E028 and/or erlotinib for 72 h, and DNA fragmentation was quantitatively measured using a cell death detection ELISA kit. Columns, mean ($n=4$); bars, S.D. Symbols: $^{*}P<0.05$; $^{**}P<0.01$; and $^{***}P<0.001$ compared with the control group. (**b** and **c**) Western blot analysis of γH2AX, caspase 3, and PARP in CL97 (**b**) and PC9/IR (**c**) cells. Cells were treated with MPT0E028 and/or erlotinib for 72 h and cell lysates were subjected to immunoblotting using the indicated antibodies. (**d** and **e**) Comparison of co-treatment with erlotinib plus MPT0E028 (**d**) or SAHA (**e**) in A549 cells. Cells were treated with the indicated drugs for 72 h, and cell lysates were subjected to immunoblotting using the indicated antibodies

MPT0E028 (Figures 6b and c). Taken together, these findings suggested that EGFR inhibition had a pivotal role in erlotinib/MPT0E028-mediated apoptotic death in TKI-resistant cells.

Co-treatment with MPT0E028 and erlotinib suppresses the growth of erlotinib-resistant tumor xenografts *in vivo*. To further evaluate the antitumor efficacy of combined treatments with MPT0E028 and an EGFR inhibitor, athymic nude mice bearing established A549 tumor xenografts were treated by oral gavage with MPT0E028 and erlotinib, both alone and in combination, for the duration of the experiment (50 days). Tumor growth was assessed by survival analysis, with survival time defined as the time for tumors to reach a volume of 1200 mm^3. Kaplan–Meier survival curves showed that the co-treated group survived significantly longer than the other treatment groups (Figure 7a). Notably, two of the seven co-treated mice displayed complete tumor regression (CR) by the end of the dosing cycle (Supplementary Figure S1). As shown in Figure 7b, treatment of the A549 NSCLC xenograft model with MPT0E028 or erlotinib alone resulted in modest inhibitions of tumor growth (by volume) compared with the vehicle-treated control. However, co-administration of

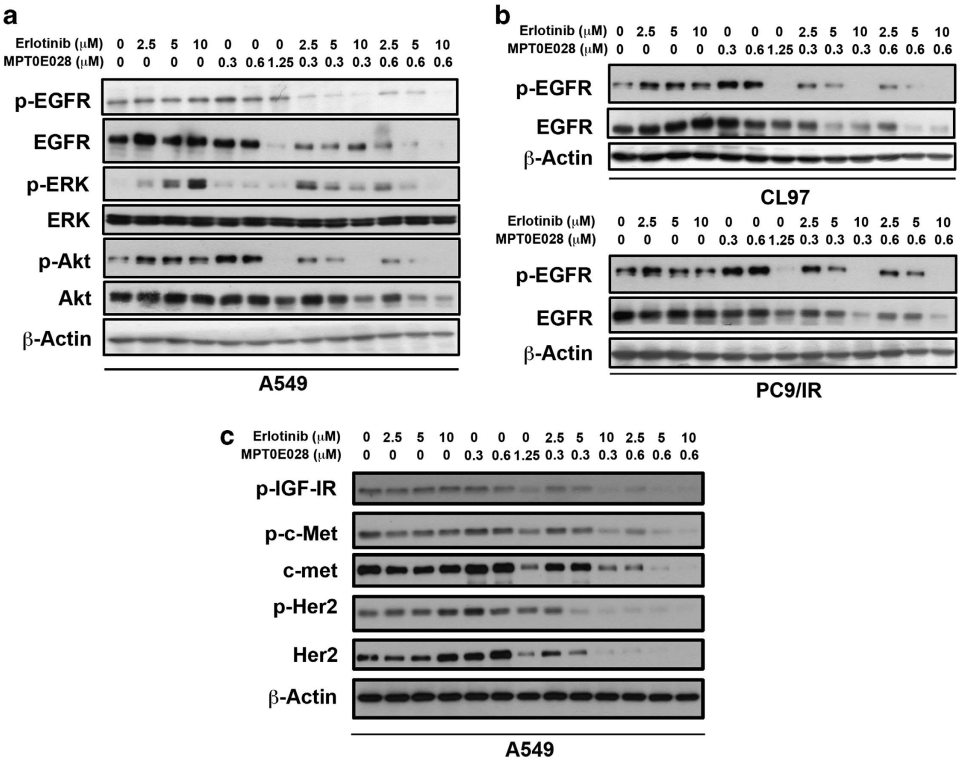

Figure 5 Significant suppression of EGFR and downstream signaling molecules is seen following co-treatment with MPT0E028 and erlotinib. (**a**) Effect of MPT0E028 and erlotinib on the activity of the EGFR/PI3K/AKT pathway in A549 cells. (**b**) Co-treatment with erlotinib and MPT0E028 downregulates phospho-EGFR and EGFR protein levels in CL97 and PC9/IR cells. (**c**) Western blot analysis of the effect of erlotinib/MPT0E028 on IGF-1R, c-met, and HER2 protein expression in A549 cells. Cells were treated with MPT0E028 and/or erlotinib for 72 h, and cell lysates were subjected to immunoblotting using the indicated antibodies

MPT0E028 and erlotinib yielded the greatest tumor growth inhibition compared with vehicle controls. Moreover, mice tolerated all of the treatments without overt signs of toxicity, as indicated by general observations of health and maintenance of body weight (Figure 7c). To correlate these *in vivo* antitumor effects with the mechanisms identified *in vitro*, we assessed intratumoral biomarkers of drug activity by immunoblotting of tumor homogenates. Our results revealed that the combined treatment markedly reduced the levels phospho-EGFR and EGFR, and elevated the levels of γH2AX, acetyl-histone H3, activated caspase 3, and PARP within tumors (Figure 7d). Taken together, our findings show that MPT0E028 exhibits promise as an agent capable of overcoming resistance to EGFR inhibitors in NSCLC.

Discussion

EGFR TKIs, such as erlotinib and gefitinib, have been found to be effective for the treatment of NSCLCs that express activating mutations of EGFR.[28,29] However, resistance to such molecular-targeted therapies occurs in some drug-resistant EGFR mutants and EGFR-wild-type tumors.[23] In order to solve this problem, new strategies have been developed against resistant mutations of EGFR, such as irreversible binding to the ATP pocket of EGFR and the selective targeting of T790M-harboring receptors.[30,31] Although these irreversible inhibitors are more potent than erlotinib against T790M, however, their clinical efficacy has been limited by pharmacokinetic issues.[32–34] In addition, phase III randomized clinical trials have shown that daily administrations of erlotinib or gefitinib in combination with conventional chemotherapy doublets have failed to improve survival in patients with advanced NSCLC.[35–37] This has led researchers to conclude that an EGFR TKI cannot be combined with cytotoxic therapies in NSCLC, and there has been little continued interest in pursuing such a strategy.

Recently, however, epigenetic therapy has emerged as a new approach for cancer treatment.[38,39] Many HDAC inhibitors, including trichostatin A, belinostat, and vorinostat, have been shown to act synergistically with numerous conventional chemotherapeutic drugs.[40–43] The broad capacity of HDAC inhibitors for synergy with various chemotherapeutic drugs indicates that they lower the threshold for cancer cells to undergo drug-mediated apoptosis. HDAC inhibitors can modulate cell responses through alterations in gene expression, induction of cell cycle arrest, inhibition of growth, and induction of apoptosis.[44] In addition, HDAC inhibitors can reduce the level of damage to normal cells and protect the body against late radiation-induced effects, such as fibrosis and secondary tumor formation.[45] Previous studies have tested some potential therapeutic strategies against lung cancer, such as the use of HDAC inhibitors to increase the sensitivity of NSCLC cell lines to gefitinib or erlotinib.[15,46]

Here, we explored the effects of the HDAC inhibitor, MPT0E028, in combination with erlotinib using *in vitro* and *in vivo* models. Synergy was consistently observed in a

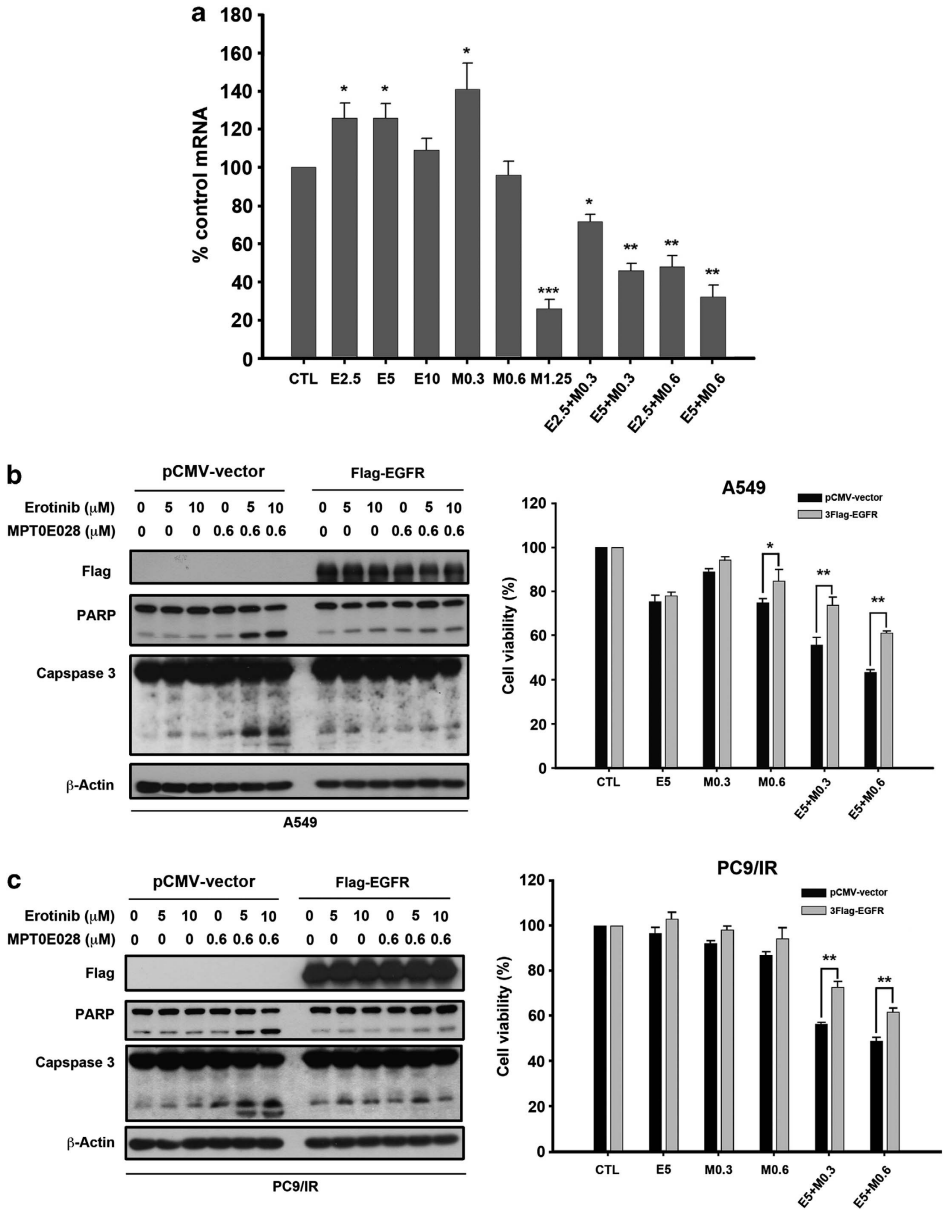

Figure 6 Evidence that EGFR involved in erlotinib/MPT0E028-mediated cell death in erlotinib-resistant cells. (**a**) mRNA expression level of EGFR in A549 cells was determined by qRT-PCR. Cells were treated with MPT0E028 (M) and/or erlotinib (E) for 72 h, and mRNA expression was analyzed by qRT-PCR as described in the Materials and Methods section. Ectopic EGFR expression protects cells against erlotinib/MPT0E028-induced cytotoxicity and apoptosis. A549 cells (**b**) and PC9/IR cells (**c**) were transfected with control vector or Flag-EGFR plasmids and treated with MPT0E028 (M) and/or erlotinib (E) as indicated for 72 h. Cell lysates were subjected to immunoblotting using the indicated antibodies (left panel) and cell viability was measured by the MTT assay (right panel). Error bars represent S.D. Symbols: $^{*}P<0.05$; $^{**}P<0.01$; and $^{***}P<0.001$ compared with the control group

number of parameters, including apoptotic protein activation, sub-G1 phase induction, and cytotoxicity. The combination of erlotinib and MPT0E028 markedly increased the degree of histone acetylation, perhaps accounting (at least in part) for these synergistic effects. Furthermore, we examined the cytotoxicity of erlotinib and MPT0E028 in different resistant cell lines: two harboring wild-type EGFR but with intrinsic resistance (A549 and H1299), two with secondary mutation T790M in EGFR (CL97 and H1975), and one (PC9/IR) with an acquired mutation of EGFR that might be contributed by epithelial-to-mesenchymal transition (EMT).[20] Our results showed that the combined treatment induced cytotoxic synergism in these resistant adenocarcinoma cell lines, suggesting that this co-treatment may overcome different types of resistance.

Preclinical data for several novel molecular-targeted inhibitors have been studied and showed dual-inhibition strategies may enhance the antitumor effects.[47] We tested the combination with MPT0E028 and selective inhibitors of RTKs such as PHA-665772 (c-met inhibitor), TAK-165 (Her2 inhibitor), and NVP-AEW541 (IGF-1R inhibitor) in A549 cells. As shown in Supplementary Figure S2, those combinations

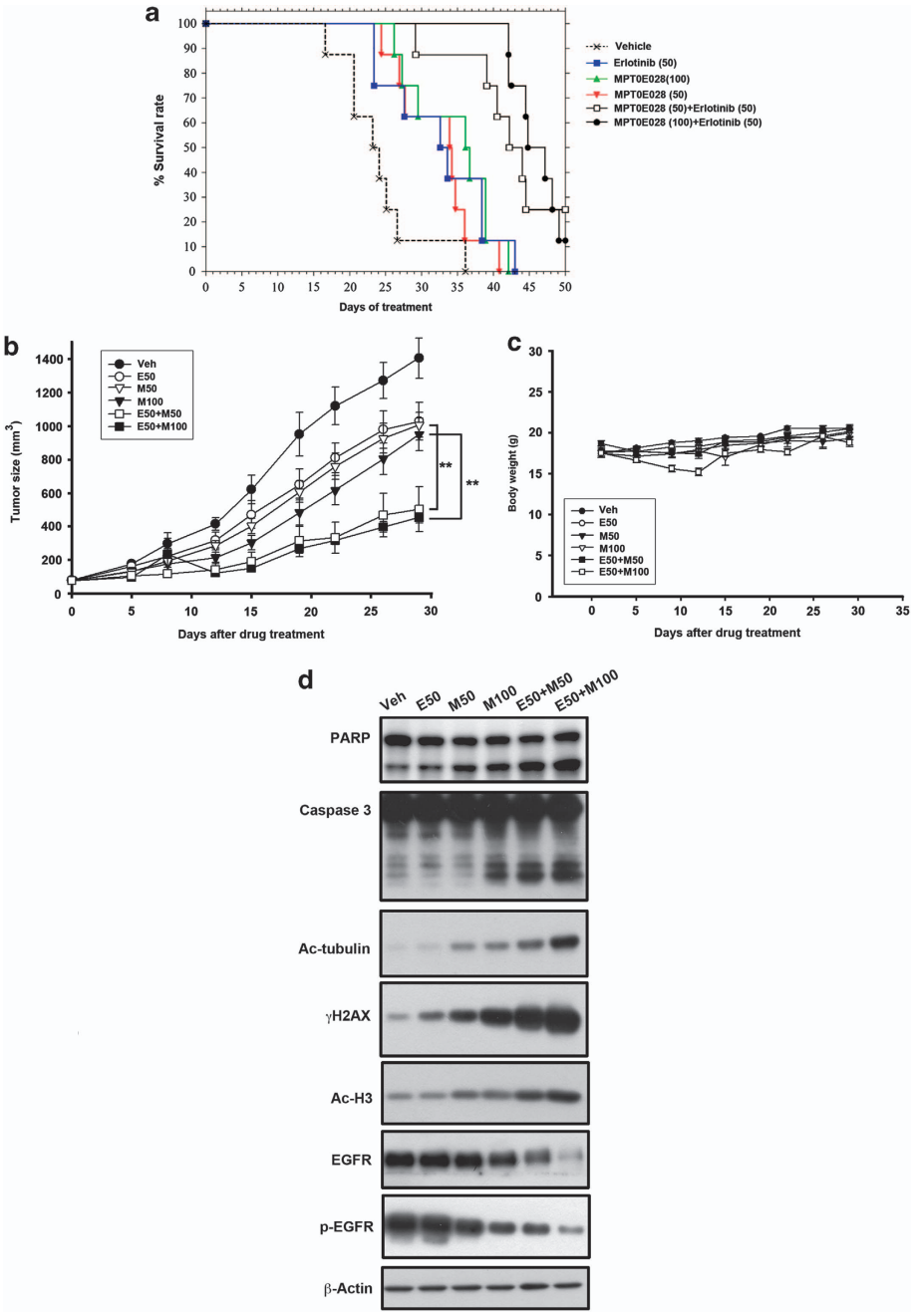

Figure 7 MPT0E028 in combination with erlotinib suppresses the growth of EGFR inhibitor-resistant tumor xenografts *in vivo*. (**a**) Kaplan–Meier survival curves are shown for each treatment group. Survival in the co-treated group was significantly extended ($P<0.05$) compared with the control groups. The log-rank test was used to calculate *P*-values. (**b**) Mice bearing established A549 tumors ($\sim 100\ mm^3$) were dosed by gavage with vehicle (Veh), MPT0E028 (M) 50 or 100 mg/kg QD, erlotinib (E) at 50 mg/kg QD, or MPT0E028 plus erlotinib at 50 + 50 mg/kg QD or 50 + 100 mg/kg QD (combination). Eight mice per group were used in the xenograft experiment. The tumor volumes of mice were measured. Symbols: $^*P<0.05$, $^{**}P<0.01$, and $^{***}P<0.001$ for comparisons with MPT0E028 alone. (**c**) The drug treatments did not cause significant body weight loss in the tested animals. (**d**) Effects of treatments on intratumoral biomarkers of drug activity in A549 xenograft tumors. Athymic nude mice bearing established subcutaneous (s.c.) A549 xenograft tumors were randomized to six groups ($n=8$ per group) that received the indicated treatments by gavage. The experimental details are described in the Materials and Methods section

did not exert significant synergistic effect (interaction) as observed in the erlotinib/MPT0E028 combination, suggesting EGFR TKI erlotinib may provide particular importance in mediating synergistic drug interactions in A549 cells.

Hyperactive Akt pathway has been associated with resistance to EGFR-TKIs in NSCLC,[48,49] suggesting that combined inhibition of Akt and EGFR signaling may be a rational and promising strategy for overcoming this resistance. Our findings support this contention by showing that treatment of EGFR inhibitor-resistant A549 cells with MPT0E028 plus erlotinib severely diminished the phosphorylation of Akt and EGFR (Figure 5a) and enhanced apoptotic

signaling (Figure 4d). Combination treatment also resulted in an increased downregulation of EGFR protein expression levels in cells (Figures 5a and b). Consequently, we found the mRNA expression level correlated with protein expression by MPT0E028 in which displayed dichotomous behavior (Figure 5a), suggesting the HDAC inhibitor MPT0E028 may activate different action of mechanisms at different concentrations. To determine the role of EGFR in erlotinib/MPT0E028 co-treatment, we ectopic expressed plasmids encoding EGFR in A549 and PC9/IR cells. Results showed that the combination treatment suppress the cell viability and induce apoptosis, at least in part, by reducing EGFR expression in cells.

Recently, studies have reported that the HDAC inhibitor vorinostat increased expression of the Bim, a BH3-only proapoptotic member of the Bcl-2 protein family, which has a crucial role in combination with gefitinib to enhance death sensitivity in the EGFR mutant, EGFR-TKI-resistant cells with the BIM deletion polymorphism.[50] We further examined the protein expression level of Bim in A549 (BIM-wild type) cells in response to erlotinib and MPT0E028. Although both of high concentrations of erlotinib and MPT0E028 slightly increased Bim_{EL} expression levels in cells, the apoptotic cell death and cell viability were not reduced in Bim knockdown cells (Supplementary Figure S3), suggesting Bim was not involved in the synergistic effect induced by combination of erlotinib and MPT0E028. Moreover, previous clinical trial indicated that combination with erlotinib and HDAC inhibitor entinostat failed to show therapeutic benefit in unselected NSCLC patients,[51] further suggesting HDAC inhibitor-induced Bim expression may have an important role in restoring cell death sensitivity of EGFR TKI in cases of NSCLC with BIM deletion polymorphism but not with wild-type BIM.

HER2 receptor overexpression occurs in 11–32% of NSCLC tumors, with increased gene copy number (amplification) documented in 2–23% of cases.[52] In addition, HER2 has a significant role in mediating the sensitivity of EGFR-mutant lung tumors to anti-EGFR therapy. A previous study identified HER2 amplification as a new mechanism through which EGFR-mutant NSCLC tumors can acquire resistance to EGFR TKIs, and found that it occurred independently of the EGFR T790M secondary mutation.[26] Recently, Guix *et al.*[27] indicated that the concomitant inhibition of both EGFR and IGF-IR was required to block PI3K signaling, and further showed that treatment of resistant cells with an IGF-IR inhibitor restored their sensitivity to EGFR TKIs. Moreover, IGF-IR signaling drives the EMT, which might have a key role in inducing acquired resistance.[20,53]

The c-Met receptor is important to a variety of malignancies, and has recently been validated as an attractive therapeutic target for the treatment of various cancers, including lung cancer.[54,55] A previous study showed that c-Met is overexpressed in up to 67% of lung adenocarcinomas and identified frequent co-expression of c-Met and EGFR in NSCLC cell lines.[21,56] Activated c-Met can interact with various other oncogenic signals, including mutant-EGFR, in maintaining and enhancing the tumor's invasive phenotype. Thus, c-Met could be a therapeutic target even in late advanced-stage metastatic disease.[57] In addition, previous reports showed the presence of signaling cross-activation between MET and EGFR in both A549 and H1975 cells,[21] and both the T790M mutation of EGFR and c-Met amplification are known mechanisms of acquired gefitinib (TKI) resistance in lung cancer.[25] As c-Met has a critical role in NSCLC, co-treatment with a c-Met inhibitor plus a reversible or irreversible EGFR kinase inhibitor (i.e., to achieve dual c-Met /EGFR inhibition) may represent an alternative strategy to circumvent T790M-EGFR-mediated resistance in lung cancer.[21]

Here, we report for the first time that erlotinib/MPT0E028 co-treatment inhibits HER-2, IGF-IR, and c-Met in erlotinib-resistant lung cancer cells. This combined treatment appears to be an effective strategy to block signaling, achieve optimized cytotoxicity, and obtain complete regression of *in vivo* xenografts. Based on these findings, we examined if the combination treatment influence the level of EGFR in nontumorous tissues. We further examined the changes of EGFR signaling in tumors and nontumorous tissues in response to combination with MPT0E028 and erlotinib. Treatment with the MPT0E028/erlotinib combination significantly reduced the phosphorylation of EGFR and EGFR in the responsive tumor cells (A549 tumor xenograft) but not in nontumorous tissues such as spleen and liver (Supplementary Figure S4), thereby providing a putative effect that MPT0E028/erlotinib combination is not toxic to normal cells. In addition, the simultaneous inhibition of RTK and HDAC pathways by erlotinib/MPT0E028 co-treatment appears to have synergistic effects on tumor suppression. These data strongly support the potential therapeutic role of a combinatorial epigenetic platform for the treatment of NSCLC, particularly in patients with TKI resistance. The established safety profiles of several combinations coupled with strong preclinical evidence should make early-phase trials a priority. Clearly, future studies will need to focus on integrating the appropriate correlative studies and seeking to identify and/or validate biomarkers of co-treatment activity in the context of disease.

Materials and Methods

Cell line and reagents. The human lung adenocarcinoma cell line CL97 was gifts from Dr. Pan-Chyr Yang (Department of Internal Medicine, National Taiwan University Hospital, Taipei, Taiwan). PC9/IR (IRRESA-resistant) clones were gifts from Dr. Chih-Hsin Yang (Graduate Institute of Oncology, Cancer Research Center, National Taiwan University, Taipei, Taiwan). A549, H1975, and H1299 cells were obtained from the American Type Culture Collection (ATCC; Manassas, VA, USA). Cells were maintained in 10% fetal bovine serum-supplemented RPMI 1640 medium (GIBCO, Grand Island, NY, USA) and 1% penicillin–streptomycin (GIBCO) at 37 °C in a humidified incubator containing 5% CO_2. Erlotinib (purity $\geqslant$ 99%) was purchased from Biovision (Milpitas, CA, USA). MPT0E028 and vorinostat (purity $\geqslant$ 98%) were synthesized by Dr. Jing-Ping Liou's Lab. Antibodies against various proteins were obtained from the following sources: PARP, Bim, anti-mouse, and anti-rabbit IgGs were obtained from Santa Cruz Biotechnology Inc. (Santa Cruz, CA, USA). Phospho-Akt (Ser473), phospho-c-Met, p-HER-2, HER-2, Akt, phospho-p44/42 MAPK (1/2 Erk) (Thr202/Tyr204), and p44/42 MAPK (1/2 Erk), were obtained from Cell Signaling (Danvers, MA, USA). Actin, phospho-IGF-IR and c-Met were from Millipore (Billerica, MA, USA). Caspase 3 was obtained from IMGENEX (San Diego, CA, USA). Flag was obtained from Sigma (St. Louis, MO, USA). NVP-AEW541 (IGF-1R inhibitor), TAK-165 (Her-2 inhibitor), and PHA-665752 (c-met inhibitor) were obtained from Selleck Chemicals (Houston, TX, USA).

Cell viability assay. Exponentially growing cells were seeded in 96-well plastic plates and exposed to serial dilutions of erlotinib, MPT0E028, or the combination treatments for 72 h. Cell viability was assayed by the

3-(4,5-dimethylthiazol-2-yl)-2,5-diphenyltetrazolium bromide assay.[58] Growth inhibition was expressed as the percentage of surviving cells in drug-treated *versus* DMSO-treated control cells (which was considered as 100% viability). The IC_{50} value was the concentration resulting in 50% cell growth inhibition by a 72-h exposure to drug(s) compared with untreated control cells and was calculated by the CompuSyn software (ComboSyn, Inc., Paramus, NJ, USA). Interactions between erlotinib and MPT0E028 were expressed as the combination index by the CompuSyn software: <1 represents synergistic cytotoxicity; 1 represents addictive cytotoxicity; and >1 represents antagonistic cytotoxicity.[59]

Clonogenic assay. Cells were plated at 800 to 1000 cells per well and exposed to DMSO or drugs at indicated concentrations for 24 h. The drugs were then washed away, and the cells were allowed to grow for 14 days. The colonies were fixed and stained with crystal violet (0.5% in 70% ethanol) and the experiments were repeated at least twice.

FACScan flow cytometric analysis. Cells were seeded in six-well plates (2.5×10^5 per well) and treated with drugs at various concentrations for indicated times. Cells were washed with phosphate-buffered saline, fixed in ice-cold 70% ethanol at $-20\,^{\circ}C$ overnight, and stained with propidium iodide (80 μg/ml) containing Triton X-100 (0.1%, v/v) and RNase A (100 μg/ml) in phosphate-buffered saline. DNA content was analyzed with the FACScan and CellQuest software (Becton Dickinson, Mountain View, CA, USA).

Immunoblotting. Cells were seeded in dishes and allowed to attach for overnight. The cells were treated with drugs for indicated concentrations. After the indicated exposure time, cells were lysed and the immunoblotting was performed as previous described.[58]

Apoptosis assay. Drug-induced apoptotic cell death was assessed using the Cell Death Detection ELISA kit (Roche Diagnostics, Basel, Switzerland). Cells were treated with drugs for 72 h. Both floating and adherent cells were collected and the assay was done according to the manufacturer's instructions.

Quantitative real-time PCR. Total RNA was isolated with TRIzol reagent by a standard protocol according to the manufacturer's protocol (Invitrogen, Carlsbad, CA, USA). mRNA (5 μg) was incubated with random primer at 65 °C for 5 min, and then reacted with M-MLV RT reagent (Promega, Madison, WI, USA) at 37 °C for 1 h to obtain cDNA. Real-time PCR was carried out by FastStart Universal SYBR Green Master (Roche, Indianapolis, IN, USA) and cDNA amplification was detected by StepOne Real-time PCR System (Applied Biosystems, Carlsbad, CA, USA). Relative gene expression was normalized to GAPDH and calculated by using the 2(–delta delta C(T)) method.[60] The primer sets were as follows: EGFR, 5′-GCGTCTCTTGCCGGAATGT-3′ and 5′-CTTGGCTCACCCTCCAGAAG-3′; GAPDH, 5′-ATTCCACCCATGGCAAATTC-3′ and 5′-TGGGATTTCCATTGATGACAAG-3′.

Transient transfection. The small interfering RNA for Bim, and negative control were purchased from Invitrogen. The Flag-EGFR plasmid and control vector (pCMV-vector) were obtained from GeneCopoeia (Rockville, MD, USA). Transfection was done using lipofectamine reagent according to the manufacturer's instructions. Following transfection, cells were allowed to recover for 24 h then started the treatment.

***In vivo* studies.** Eight-week-old female nude-athymic mice were group-housed under conditions of constant photoperiod (12-h light/12-h dark at 21–23 °C and 60–85% humidity) with *ad libitum* access to sterilized food and water. All animal experiments followed ethical standards, and protocols have been reviewed and approved by Animal Use and Management Committee of National Taiwan University (IACUC approval no: 20100225). Each mouse was inoculated s.c. with 1×10^6 A549 cells in a total volume of 0.1 ml serum-free medium containing 50% Matrigel (BD Biosciences, Franklin Lakes, NJ, USA). As tumors became established ($\sim 100\,mm^3$), mice were randomized to four groups ($n = 8$) that received the following treatments: (a) 0.5% carboxymethyl cellulose/0.1%Tween 80 vehicle, (b) MPT0E028 at 50 or 100 mg/kg/day, (c) erlotinib at 50 mg/kg/day, and (d) MPT0E028 plus erlotinib at 50 + 50 mg/kg/day or 50 + 100 mg/kg/day. Mice received treatments by gavage for the duration of the study. Tumors were measured weekly using calipers. Tumor size, in mm^3, was calculated from: where w = width and l = length in mm of the tumor. Tumor volume = $(w^2 \times l)/2$. A portion of each tumor was frozen in liquid nitrogen for western blotting analysis.

Statistics and data analysis. Each experiment was performed at least three times, and presentative data are shown. Data in bar graph are given as the means ± S.D. Means were checked for statistical difference using the *t*-test and *P*-values <0.05 were considered significant (*$P<0.05$, **$P<0.01$, ***$P<0.001$). In animal xenograft models, the log-rank test was used to determine the statistical significance of the difference between the time to end point values of two groups, except any (non-treatment-related) deaths. Statistical and graphical analyses were performed with Prism 3.03 (GraphPad, La Jolla, CA, USA) for Windows. The two-tailed statistical analyses were conducted at $P = 0.05$. Kaplan–Meier plots show the percentage of animals remaining in the study *versus* time. The Kaplan–Meier plots use the same data set as the log-rank test.

Conflict of Interest

The authors declare no conflict of interest.

Acknowledgements. We thank Dr. Pan-Chyr Yang and Dr. Chih-Hsin Yang for providing CL97 and PC9/IR cells in our study. This study was supported by grants from the National Science Council of Taiwan NSC 99-2320-B400-008-MY3, NSC 99-2628-B002-024-MY3, NSC 100-2628-M038-001-MY3, and NSC 101-2325-B038-004-CC2.

1. Hynes NE, Lane HA. ERBB receptors and cancer: the complexity of targeted inhibitors. *Nat Rev Cancer* 2005; **5**: 341–354.
2. Mendelsohn J, Baselga J. Status of epidermal growth factor receptor antagonists in the biology and treatment of cancer. *J Clin Oncol* 2003; **21**: 2787–2799.
3. Garnis C, Lockwood WW, Vucic E, Ge Y, Girard L, Minna JD *et al.* High resolution analysis of non-small cell lung cancer cell lines by whole genome tiling path array CGH. *Int J Cancer* 2006; **118**: 1556–1564.
4. Yokota J, Kohno T. Molecular footprints of human lung cancer progression. *Cancer Sci* 2004; **95**: 197–204.
5. Pao W, Chmielecki J. Rational, biologically based treatment of EGFR-mutant non-small-cell lung cancer. *Nat Rev Cancer* 2010; **10**: 760–774.
6. Wang Y, Rouggly L, You M, Lubet R. Animal models of lung cancer characterization and use for chemoprevention research. *Prog Mol Biol Transl Sci* 2012; **105**: 211–226.
7. Breathnach OS, Freidlin B, Conley B, Green MR, Johnson DH, Gandara DR *et al.* Twenty-two years of phase III trials for patients with advanced non-small-cell lung cancer: sobering results. *J Clin Oncol* 2001; **19**: 1734–1742.
8. Tokumo M, Toyooka S, Kiura K, Shigematsu H, Tomii K, Aoe M *et al.* The relationship between epidermal growth factor receptor mutations and clinicopathologic features in non-small cell lung cancers. *Clin Cancer Res* 2005; **11**: 1167–1173.
9. Tsao MS, Sakurada A, Cutz JC, Zhu CQ, Kamel-Reid S, Squire J *et al.* Erlotinib in lung cancer—molecular and clinical predictors of outcome. *N Engl J Med* 2005; **353**: 133–144.
10. Pao W, Miller VA, Politi KA, Riely GJ, Somwar R, Zakowski MF *et al.* Acquired resistance of lung adenocarcinomas to gefitinib or erlotinib is associated with a second mutation in the EGFR kinase domain. *PLoS Med* 2005; **2**: e73.
11. Kobayashi S, Boggon TJ, Dayaram T, Janne PA, Kocher O, Meyerson M *et al.* EGFR mutation and resistance of non-small-cell lung cancer to gefitinib. *N Engl J Med* 2005; **352**: 786–792.
12. Pao W, Wang TY, Riely GJ, Miller VA, Pan Q, Ladanyi M *et al.* KRAS mutations and primary resistance of lung adenocarcinomas to gefitinib or erlotinib. *PLoS Med* 2005; **2**: e17.
13. Bolden JE, Peart MJ, Johnstone RW. Anticancer activities of histone deacetylase inhibitors. *Nat Rev Drug Discov* 2006; **5**: 769–784.
14. LaBonte MJ, Wilson PM, Fazzone W, Russell J, Louie SG, El-Khoueiry A *et al.* The dual EGFR/HER2 inhibitor lapatinib synergistically enhances the antitumor activity of the histone deacetylase inhibitor panobinostat in colorectal cancer models. *Cancer Res* 2011; **71**: 3635–3648.
15. Lai CJ, Bao R, Tao X, Wang J, Atoyan R, Qu H *et al.* CUDC-101, a multitargeted inhibitor of histone deacetylase, epidermal growth factor receptor, and human epidermal growth factor receptor 2, exerts potent anticancer activity. *Cancer Res* 2010; **70**: 3647–3656.
16. Busser B, Sancey L, Josserand V, Niang C, Khochbin S, Favrot MC *et al.* Amphiregulin promotes resistance to gefitinib in nonsmall cell lung cancer cells by regulating Ku70 acetylation. *Mol Ther* 2010; **18**: 536–543.
17. Thurn KT, Thomas S, Moore A, Munster PN. Rational therapeutic combinations with histone deacetylase inhibitors for the treatment of cancer. *Future Oncol* 2011; **7**: 263–283.
18. Huang HL, Lee HY, Tsai AC, Peng CY, Lai MJ, Wang JC *et al.* Correction: anticancer activity of MPT0E028, a novel potent histone deacetylase inhibitor, in human colorectal cancer HCT116 cells *in vitro* and *in vivo*. *PLoS One* 2012; **7**: e43645.
19. Yeh CT, Wu AT, Chang PM, Chen KY, Yang CN, Yang SC *et al.* Trifluoperazine, an antipsychotic agent, inhibits cancer stem cell growth and overcomes drug resistance of lung cancer. *Am J Respir Crit Care Med* 2012; **186**: 1180–1188.

20. Chang TH, Tsai MF, Su KY, Wu SG, Huang CP, Yu SL *et al.* Slug confers resistance to the epidermal growth factor receptor tyrosine kinase inhibitor. *Am J Respir Crit Care Med* 2011; **183**: 1071–1079.
21. Tang Z, Du R, Jiang S, Wu C, Barkauskas DS, Richey J *et al.* Dual MET-EGFR combinatorial inhibition against T790M-EGFR-mediated erlotinib-resistant lung cancer. *Br J Cancer* 2008; **99**: 911–922.
22. Li T, Ling YH, Goldman ID, Perez-Soler R. Schedule-dependent cytotoxic synergism of pemetrexed and erlotinib in human non-small cell lung cancer cells. *Clin Cancer Res* 2007; **13**: 3413–3422.
23. Sharma SV, Bell DW, Settleman J, Haber DA. Epidermal growth factor receptor mutations in lung cancer. *Nat Rev Cancer* 2007; **7**: 169–181.
24. Hidalgo M, Siu LL, Nemunaitis J, Rizzo J, Hammond LA, Takimoto C *et al.* Phase I and pharmacologic study of OSI-774, an epidermal growth factor receptor tyrosine kinase inhibitor, in patients with advanced solid malignancies. *J Clin Oncol* 2001; **19**: 3267–3279.
25. Engelman JA, Zejnullahu K, Mitsudomi T, Song Y, Hyland C, Park JO *et al.* MET amplification leads to gefitinib resistance in lung cancer by activating ERBB3 signaling. *Science* 2007; **316**: 1039–1043.
26. Takezawa K, Pirazzoli V, Arcila ME, Nebhan CA, Song X, de Stanchina E *et al.* HER2 amplification: a potential mechanism of acquired resistance to EGFR inhibition in EGFR-mutant lung cancers that lack the second-site EGFRT790M mutation. *Cancer Discov* 2012; **2**: 922–933.
27. Guix M, Faber AC, Wang SE, Olivares MG, Song Y, Qu S *et al.* Acquired resistance to EGFR tyrosine kinase inhibitors in cancer cells is mediated by loss of IGF-binding proteins. *J Clin Invest* 2008; **118**: 2609–2619.
28. Pao W, Miller VA. Epidermal growth factor receptor mutations, small-molecule kinase inhibitors, and non-small-cell lung cancer: current knowledge and future directions. *J Clin Oncol* 2005; **23**: 2556–2568.
29. Janne PA, Johnson BE. Effect of epidermal growth factor receptor tyrosine kinase domain mutations on the outcome of patients with non-small cell lung cancer treated with epidermal growth factor receptor tyrosine kinase inhibitors. *Clin Cancer Res* 2006; **12**: 4416s–4420s.
30. Li D, Ambrogio L, Shimamura T, Kubo S, Takahashi M, Chirieac LR *et al.* BIBW2992, an irreversible EGFR/HER2 inhibitor highly effective in preclinical lung cancer models. *Oncogene* 2008; **27**: 4702–4711.
31. Zhou W, Ercan D, Chen L, Yun CH, Li D, Capelletti M *et al.* Novel mutant-selective EGFR kinase inhibitors against EGFR T790M. *Nature* 2009; **462**: 1070–1074.
32. Wong KK. HKI-272 in non small cell lung cancer. *Clin Cancer Res* 2007; **13**: s4593–s4596.
33. Eskens FA, Mom CH, Planting AS, Gietema JA, Amelsberg A, Huisman H *et al.* A phase I dose escalation study of BIBW 2992, an irreversible dual inhibitor of epidermal growth factor receptor 1 (EGFR) and 2 (HER2) tyrosine kinase in a 2-week on, 2-week off schedule in patients with advanced solid tumours. *Br J Cancer* 2008; **98**: 80–85.
34. Sos ML, Rode HB, Heynck S, Peifer M, Fischer F, Kluter S *et al.* Chemogenomic profiling provides insights into the limited activity of irreversible EGFR Inhibitors in tumor cells expressing the T790M EGFR resistance mutation. *Cancer Res* 2010; **70**: 868–874.
35. Herbst RS, Prager D, Hermann R, Fehrenbacher L, Johnson BE, Sandler A *et al.* TRIBUTE: a phase III trial of erlotinib hydrochloride (OSI-774) combined with carboplatin and paclitaxel chemotherapy in advanced non-small-cell lung cancer. *J Clin Oncol* 2005; **23**: 5892–5899.
36. Giaccone G, Herbst RS, Manegold C, Scagliotti G, Rosell R, Miller V *et al.* Gefitinib in combination with gemcitabine and cisplatin in advanced non-small-cell lung cancer: a phase III trial–INTACT 1. *J Clin Oncol* 2004; **22**: 777–784.
37. Herbst RS, Giaccone G, Schiller JH, Natale RB, Miller V, Manegold C *et al.* Gefitinib in combination with paclitaxel and carboplatin in advanced non-small-cell lung cancer: a phase III trial–INTACT 2. *J Clin Oncol* 2004; **22**: 785–794.
38. Minucci S, Pelicci PG. Histone deacetylase inhibitors and the promise of epigenetic (and more) treatments for cancer. *Nat Rev Cancer* 2006; **6**: 38–51.
39. Kristensen LS, Nielsen HM, Hansen LL. Epigenetics and cancer treatment. *Eur J Pharmacol* 2009; **625**: 131–142.
40. Arnold NB, Arkus N, Gunn J, Korc M. The histone deacetylase inhibitor suberoylanilide hydroxamic acid induces growth inhibition and enhances gemcitabine-induced cell death in pancreatic cancer. *Clin Cancer Res* 2007; **13**: 18–26.
41. Dowdy SC, Jiang S, Zhou XC, Hou X, Jin F, Podratz KC *et al.* Histone deacetylase inhibitors and paclitaxel cause synergistic effects on apoptosis and microtubule stabilization in papillary serous endometrial cancer cells. *Mol Cancer Ther* 2006; **5**: 2767–2776.
42. Rikiishi H, Shinohara F, Sato T, Sato Y, Suzuki M, Echigo S. Chemosensitization of oral squamous cell carcinoma cells to cisplatin by histone deacetylase inhibitor, suberoylanilide hydroxamic acid. *Int J Oncol* 2007; **30**: 1181–1188.
43. Kim MS, Blake M, Baek JH, Kohlhagen G, Pommier Y, Carrier F. Inhibition of histone deacetylase increases cytotoxicity to anticancer drugs targeting DNA. *Cancer Res* 2003; **63**: 7291–7300.
44. Muhlethaler-Mottet A, Flahaut M, Bourloud KB, Auderset K, Meier R, Joseph JM *et al.* Histone deacetylase inhibitors strongly sensitise neuroblastoma cells to TRAIL-induced apoptosis by a caspases-dependent increase of the pro- to anti-apoptotic proteins ratio. *BMC Cancer* 2006; **6**: 214.
45. Chung YL, Wang AJ, Yao LF. Antitumor histone deacetylase inhibitors suppress cutaneous radiation syndrome: implications for increasing therapeutic gain in cancer radiotherapy. *Mol Cancer Ther* 2004; **3**: 317–325.
46. Witta SE, Gemmill RM, Hirsch FR, Coldren CD, Hedman K, Ravdel L *et al.* Restoring E-cadherin expression increases sensitivity to epidermal growth factor receptor inhibitors in lung cancer cell lines. *Cancer Res* 2006; **66**: 944–950.
47. Wick W, Weller M, Weiler M, Batchelor T, Yung AW, Platten M. Pathway inhibition: emerging molecular targets for treating glioblastoma. *Neuro Oncol* 2011; **13**: 566–579.
48. Brognard J, Clark AS, Ni Y, Dennis PA. Akt/protein kinase B is constitutively active in non-small cell lung cancer cells and promotes cellular survival and resistance to chemotherapy and radiation. *Cancer Res* 2001; **61**: 3986–3997.
49. Janmaat ML, Kruyt FA, Rodriguez JA, Giaccone G. Response to epidermal growth factor receptor inhibitors in non-small cell lung cancer cells: limited antiproliferative effects and absence of apoptosis associated with persistent activity of extracellular signal-regulated kinase or Akt kinase pathways. *Clin Cancer Res* 2003; **9**: 2316–2326.
50. Nakagawa T, Takeuchi S, Yamada T, Ebi H, Sano T, Nanjo S *et al.* EGFR-TKI resistance due to BIM polymorphism can be circumvented in combination with HDAC inhibition. *Cancer Res* 2013; **73**: 2428–2434.
51. Witta SE, Jotte RM, Konduri K, Neubauer MA, Spira AI, Ruxer RL *et al.* Randomized phase II trial of erlotinib with and without entinostat in patients with advanced non-small-cell lung cancer who progressed on prior chemotherapy. *J Clin Oncol* 2012; **30**: 2248–2255.
52. Swanton C, Futreal A, Eisen T. Her2-targeted therapies in non-small cell lung cancer. *Clin Cancer Res* 2006; **12**: 4377s–4383s.
53. Kim HJ, Litzenburger BC, Cui X, Delgado DA, Grabiner BC, Lin X *et al.* Constitutively active type I insulin-like growth factor receptor causes transformation and xenograft growth of immortalized mammary epithelial cells and is accompanied by an epithelial-to-mesenchymal transition mediated by NF-kappaB and snail. *Mol Cell Biol* 2007; **27**: 3165–3175.
54. Garcia S, Dales JP, Jacquemier J, Charafe-Jauffret E, Birnbaum D, Andrac-Meyer L *et al.* c-Met overexpression in inflammatory breast carcinomas: automated quantification on tissue microarrays. *Br J Cancer* 2007; **96**: 329–335.
55. Ma PC, Kijima T, Maulik G, Fox EA, Sattler M, Griffin JD *et al.* c-MET mutational analysis in small cell lung cancer: novel juxtamembrane domain mutations regulating cytoskeletal functions. *Cancer Res* 2003; **63**: 6272–6281.
56. Ma PC, Jagadeeswaran R, Jagadeesh S, Tretiakova MS, Nallasura V, Fox EA *et al.* Functional expression and mutations of c-Met and its therapeutic inhibition with SU11274 and small interfering RNA in non-small cell lung cancer. *Cancer Res* 2005; **65**: 1479–1488.
57. Comoglio PM, Giordano S, Trusolino L. Drug development of MET inhibitors: targeting oncogene addiction and expedience. *Nat Rev Drug Discov* 2008; **7**: 504–516.
58. Chen MC, Pan SL, Shi Q, Xiao Z, Lee KH, Li TK *et al.* QS-ZYX-1-61 induces apoptosis through topoisomerase II in human non-small-cell lung cancer A549 cells. *Cancer Sci* 2012; **103**: 80–87.
59. Chou TC. Drug combination studies and their synergy quantification using the Chou-Talalay method. *Cancer Res* 2010; **70**: 440–446.
60. Livak KJ, Schmittgen TD. Analysis of relative gene expression data using real-time quantitative PCR and the 2(-delta delta C(T)) method. *Methods* 2001; **25**: 402–408.

Supplementary Information accompanies this paper on Cell Death and Disease website (http://www.nature.com/cddis)